Chemical Engineering and Processing 62 (2012) 69–77

Contents lists available at SciVerse ScienceDirect

Chemical Engineering and Processing: Process Intensification

journal homepage: www.elsevier.com/locate/cep

Continuous synthesis of functional silver nanoparticles using microreactor: Effect of surfactant and process parameters

G.A. Patil[c], M.L. Bari[c], B.A. Bhanvase[a], Vivek Ganvir[b], S. Mishra[c], S.H. Sonawane[d,*]

[a] Chemical Engineering Department, Vishwakarma Institute of Technology, Pune, India
[b] Tata Consultancy Services, Pune, India
[c] University Department of Chemical Technology, North Maharashtra University, Jalgaon, India
[d] Chemical Engineering Department, National Institute of Technology Warangal, India

ARTICLE INFO

Article history:
Received 20 September 2011
Received in revised form 14 March 2012
Accepted 14 September 2012
Available online 24 September 2012

Keywords:
Microreactor
Batch process
Silver nanoparticles
Particle size distribution
RTD

ABSTRACT

In this work an attempt was made to intensify the process of nanoparticles synthesis in microreactor. Main objective of the work was to investigate the intensification of silver nanoparticles synthesis using surfactants and to study the effect of associated process parameters in microreactor such as concentration and flow rate of precursor. Reduction reaction was carried out using silver nitrate and sodium borohydride. Two surfactants namely sodium dodecyl sulfate (SDS) and N-cetyl N,N,N,trimethyl ammonium bromide (CTAB) were used to evaluate the effect on particle size by controlling nucleation and growth mechanism. Results of microreactor synthesis were compared with batch process.

Optimum parameters such as flow rates, concentrations of reactants/surfactants were determined to obtain nanosize silver colloidal particles in continuous microreactor. Results show that use of 0.02 g/mL SDS with 1 mL/min (0.001 M) $AgNO_3$ and 3 mL/min (0.003 M) $NaBH_4$ flow rate shows minimum particle size of 4.8 nm. From residence time distribution (RTD) data, it is found that the Pe_{ax} number was highest 0.39 at *Re* number 67 (flow rate of 7 mL/min), which signifies the less axial dispersion. The increase in the particle size with an increase in the CTAB loading is due to the agglomeration effect that cationic CTAB, which has positive charge on head, leads to aggregation. SDS favors the reduction in particle size of silver nanoparticle.

1. Introduction

Production of mono dispersed colloidal nanoparticles has become an important research subject in recent years, as colloidal particles exhibit unique optical, electronic and magnetic properties, which make them ideal candidates for engineering applications. Colloidal nanoparticles find applications in different areas such as catalysis, biological tags, gene detection, targeted drug delivery system, antimicrobial additives, conducting inks [1–5]. Properties and the applications of these nanoparticles depend upon the shape, size and distribution of nanoparticles [6]. Hence, nanoparticles synthesis by micro fluidic device has gained major interest in recent years. Further, batch synthesis involves the atom-by-atom particle growth by using precipitation process. Hence particle size and particle size distributions are usually wide in case of batch synthesis. It is also important to note that down stream processing is needed to extract the desired particle size in such batch process [7]. Particle size obtained in microreactors has smaller and narrow particle size distribution than batch process due to better mixing and mass transfer in microfluidic devices [5]. Microreactor devices offer higher surface to volume ratio compared to the batch reactors hence the removal of heat is effectively carried out for exothermic reactions. Microfluidics has been used not only for synthesis of inorganic, organic and biological materials but also for synthesis of the janus, polymeric nanoparticles and hybrid materials. In microreactor systems, reaction takes place in small reaction volume, hence there is less heat and mass transfer resistances which help in safe handling of exothermic reactions. Rapid mixing of reactants and control of reagent concentration can produce precise conditions which are required for nanoparticle synthesis. Mixing of reactants in microreactor takes place very rapidly and control of reagent concentration can produce precise conditions which are required for nanoparticle synthesis. Hybrid nanoparticles are also synthesized by microreactor technology and particle size can be manipulated at the fluid–fluid interfaces in microreactors [8–16].

Boleininger et al. [17] synthesized the gold/silver metal nanorods using ascorbic acid, CTAB solution and precursor such as $HAuCl_4/AgNO_3$. In presence of CTAB, prepared micelles were used as template for anisotropic growth of particles. In batch synthesis

* Corresponding authors. Tel.: +91 870 2462626.
E-mail addresses: profsm@rediffmail.com (S. Mishra), shirishsonawane@rediffmail.com, shirishsonawane09@gmail.com (S.H. Sonawane).

0255-2701/$ – see front matter © 2012 Elsevier B.V. All rights reserved.
http://dx.doi.org/10.1016/j.cep.2012.09.007

process, they found that initial particles act as seeds, which increases the overall particle size. While, in microreactor synthesis the seeding of particles is being avoided by maintaining small residence time in the microreactor [17]. Lin et al. [18] demonstrate the synthesis of mono dispersed silver nanoparticles using single precursor pentafluoropropionate. They studied the effect of temperature, flow rates, reaction time and reported the use of single precursor for the preparation of monodisperse nanoparticles of silver [18]. Number of articles report on synthesis of gold and silver metal and metal oxide and other nanoparticles using microreactor technology [19–26]. Gold and silver nanoparticles synthesis using a polydimethylsiloxane (PDMS) in microreactor by reduction reaction between metal salt solutions and borohydride with tri-sodium citrate as the capping agent was carried out by Singh et al. [19]. Wagner and Köhler [20] synthesized gold nanoparticles by citrate reduction reaction in microreactor. They have used polyvinyl pyrrolidone for stabilization of particles. They found that mean particle size increases with decreasing flow rate, and also observed that with if the gold ions concentration is equal to seed concentration, then particle growth is observed. Wagner et al. [21] in other article [21] synthesized spherical gold nanoparticles with the size range from 5 to 50 nm by using gold precursor and ascorbic acid, and they have used different flow rates. They found that by doubling the flow rate a reduction in narrow size is achieved in comparison to batch synthesis [21]. Jeevarathinam et al. [27] synthesized the barium sulfate nanoparticles by reacting barium chloride and sodium sulfate solutions by precipitation reaction. They found that mixing is a very important parameter in such precipitation reactions carried out in microreactor. The particle size is found to be reduced because of local mixing, which gives higher local nucleation results in the reduction in particle size distribution. They also observed that with decreasing the flow rate of barium chloride the particle size is found to be reduced.

In this manuscript, we report the process parameters affecting microreactor based colloidal nano particle synthesis and role of surfactant for intensification of process. Further, it has also been compared with the batch process. In this work, linear low-density polyethylene (LLDPE) based spiral microreactor has been used which offers better mixing over metal based microreactors. Optimum parameters such as flow rates, concentrations of reactants/surfactants were determined to obtain nanosize silver colloidal particles in continuous microreactor. Conversion of reaction was monitored by using UV spectra of the sample. In this work we have demonstrated the continuous production of silver nano particles with narrow size distribution.

2. Experimental methodology

2.1. Materials

Silver nitrate ($AgNO_3$, 99%) of analytical grade was procured from Merck Specialties Pvt. Ltd., Mumbai. Analytical grade sodium borohydride (99%, $NaBH_4$) and sodium dodecyl sulfate (SDS, $C_{12}H_{25}SO_4Na$, 99%) were procured from Thomas Baker (Chemical) Ltd. N-cetyl-N,N,N trimethyl ammonium bromide (CTAB, 99%) was procured from Sigma Aldrich. Millipore deionized water (resistivity > 1 MΩ cm) was used for preparation of all aqueous solutions.

2.2. Synthesis of silver nanoparticles in batch process and microreactor

Chemical reduction method was used for synthesis of silver nanoparticles. As shown in reaction scheme (1), sodium borohydride and silver nitrate were reacted to form silver nanoparticles. If reaction is carried out in presence of suitable surfactant, surface of particles will be covered and particles remain in stable form

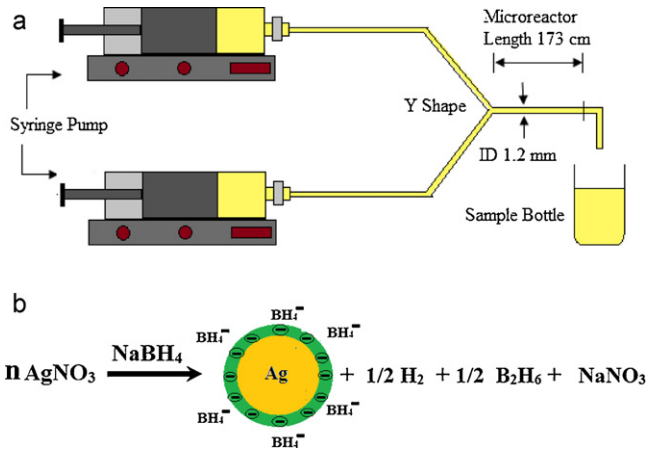

Fig. 1. (a) Schematic diagram of the experimental set-up for synthesis of silver nanoparticles in microreactor. (b) Reduction reaction to generate silver colloidal particles synthesized in presence of surfactant.

without aggregation. The charges present on the surface of these nanoparticles determine the stability of particles to remain in colloidal form which is depicted in Fig. 1a.

$$AgNO_3 + NaBH_4 \rightarrow Ag^0 + \tfrac{1}{2}H_2 + \tfrac{1}{2}B_2H_6 + NaNO_3 \quad (1)$$

In typical batch experiment, 20 mL of silver nitrate (0.001 M) and 60 mL sodium borohydride (0.002 M) each containing SDS (0.1 g) were prepared in separate flask. Initially, these solutions were cooled (10 °C) in an ice bath then the solutions were added in batch reactor. Reaction was carried out using magnetic stirrer and progress of reaction was monitored by UV analysis. In other experiments, in place of SDS, precursor solutions were prepared using CTAB surfactant as described earlier.

Microreactor was fabricated using linear low density polyethylene tube (LLDPE) having 173 cm length and 1.2 mm inner diameter. Two syringe needles were inserted in the spiral shape microreactor making Y shape geometry and synthesis of colloidal silver nanoparticles were carried out in it. Molar concentration of silver nitrate and sodium borohydride solutions were varied from 0.001 to 0.005 in different experiments. Sodium borohydride solutions were cooled in ice bath up to 10 °C for 20 min. SDS was added in both precursors (0.02 g). Both solutions were filled in two separate syringes (50 mL each, UNIEM Mumbai, India) and were mounted on syringe pump. The flow rate of $AgNO_3$ solution was set at 1 mL/min and 3 mL/min for $NaBH_4$ solution. The $NaBH_4$ used was in excess in order to reduce the ionic silver and to stabilize the silver nanoparticles.

Both precursors passed through spiral microreactor, and the product was collected in glass vials. Initially, faint yellow color of colloidal solution appeared and then clear yellow solution was formed when final product was obtained. Conversion of reaction mixture was monitored by taking UV spectra at an interval of 1 min. Yellow color and highest peak observed in UV spectrum confirm the complete formation of silver nanoparticles. Fig. 1b depicts a schematic diagram of the experimental setup. Another surfactant, CTAB (0.02 g) was used and the above procedure was repeated for synthesis of Ag^0 nanoparticles in microreactor.

2.3. Residence time distribution in microreactor

For the RTD measurements, tracer input was carried out using pulse input method and the output concentration of the tracer was monitored at the outlet of the microreactor. RTD experiments were accomplished in a flow rate range between 3 and 7 mL/min of water.

Fig. 2. Colloidal silver in different stages for microreactor, (A) grayish precipitate without surfactant, (B) clear yellow sol at initial stage using surfactant, (C) dark yellow sol at final stage using surfactant ($AgNO_3$ flow rate = 1 mL/min, $NaBH_4$ flow rate = 3 mL/min, space time τ = 0.48 min). (For interpretation of the references to color in this figure legend, the reader is referred to the web version of the article.)

After stabilization of system a 10 mL pulse input of 0.1 N NaOH solutions of tracer outlet concentration was monitored. The pulse input was maintained at 0.5 s using a syringe. The tracer analysis was carried out by measuring the output concentration of NaOH solution of the microreactor using acid base titration.

2.4. Characterization

UV spectra of sample were taken in definite time intervals using UV spectrophotometer (SHIMADZU 160A model). From UV absorption spectra λ_{max} value was found to be 402 nm for the formation of silver nanoparticles. Dynamic light-scattering (DLS Malvern Instruments Ltd., USA) was used for measurements of particle size distribution. TEM of the samples were carried out using a CM200, PHILIPS Microscopy (20–200 kV, resolution 2.4 Å and magnification 1,000,000×).

3. Results and discussion

3.1. Mechanism of silver nanoparticles formation

The reduction reaction (Eq. (1)) leads to formation of silver atoms that are more stable and act as the nuclei for formation of aggregates. These particles may dissociate or they will grow. Once this embryo reaches its critical size, it tends to get separated from the solution as solid particles and these particles called as 'nuclei'. These nuclei preliminarily grow to nanosize, if further silver atoms are added. The mechanism is such that the growth and aggregation occur simultaneously. To obtain stable yellow colloidal silver with desired yield and narrow size, reaction conditions such as stirring time and relative quantities of precursor (both their relative molarities and the absolute number of moles of each reactant) must be carefully controlled [18]. Formation of silver nanoparticles can be observed by a change in color, since small nanoparticles of silver show yellow color. Further, yellow color changes to dark gray indicates the formation of aggregates and wide particle size distribution. Appearance of dark gray color of solution indicates that the particle growth has occurred by aggregation mechanism. While yellow color of solution indicates the formation of the stabilized colloidal particles [28]. Fig. 2a shows the different colloidal nanoparticles obtained with and without surfactant through microreactor. Fig. 2a indicates formation of grayish precipitate without surfactant and Fig. 2b (results at, τ < 0.48 min).

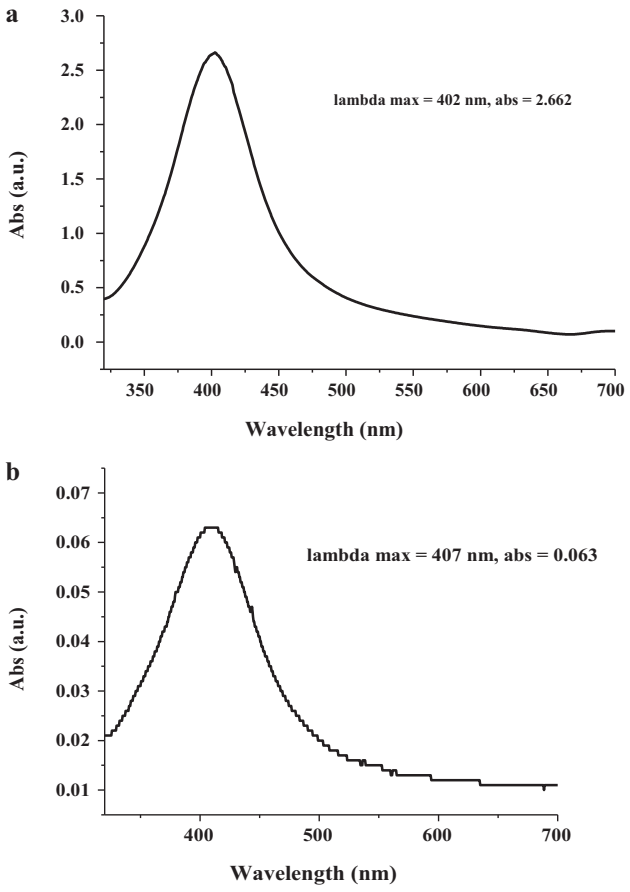

Fig. 3. (a) UV absorption spectrum of clear yellow colloidal Ag^0 in microreactor. (b) UV absorption spectrum of clear yellow colloidal Ag^0 in batch reactor.

Fig. 2c shows, the yellow color indicating the stabilized nano silver particles due to presence of surfactant. These experimental results were obtained by maintaining $AgNO_3$ precursor solution addition rate at 1 mL/min and 3 mL/min for $NaBH_4$ (space time of reaction was maintained at τ = 0.48 min).

3.2. Effect of batch and microreactor process

The reduction reaction was carried out in batch and microreactor to determine the effect on the particle size. Fig. 3a and b shows UV absorption spectrum of clear yellow colloidal silver (Ag^0) obtained in microreactor ($AgNO_3$ flow rate 0.83 mL/min and $NaBH_4$ at 2.5 mL/min, at τ = 0.58 min) and in batch reactor respectively. As shown in Fig. 3a and b, the absorbance values of Ag^0 nanoparticles synthesized by microreactor and batch reactor technique were found to be 2.66 and 0.063 respectively. More value of absorbance indicates the generation of more number of nuclei in microreactor synthesis process. It is known that the more the value of peak width at half maximum (PWHM); the more is the value of particle size distribution of nanoparticles. Also the particles size increases with the increase in λ_{max} value [29–36]. The silver nanoparticles synthesized in current study indicate formation of small particle size as compared to batch processes reported in literature. In the present study, the particle size obtained was in the range of 3–7 nm in microreactor and it was confirmed by TEM images as shown in Fig. 4a with PWHM 69. The obtain results indicates that the particle size attained in microreactors has narrow particle size distribution. Moreover the TEM images in Fig. 4a and b conformed that the silver nano particles achieved spherical shape while that

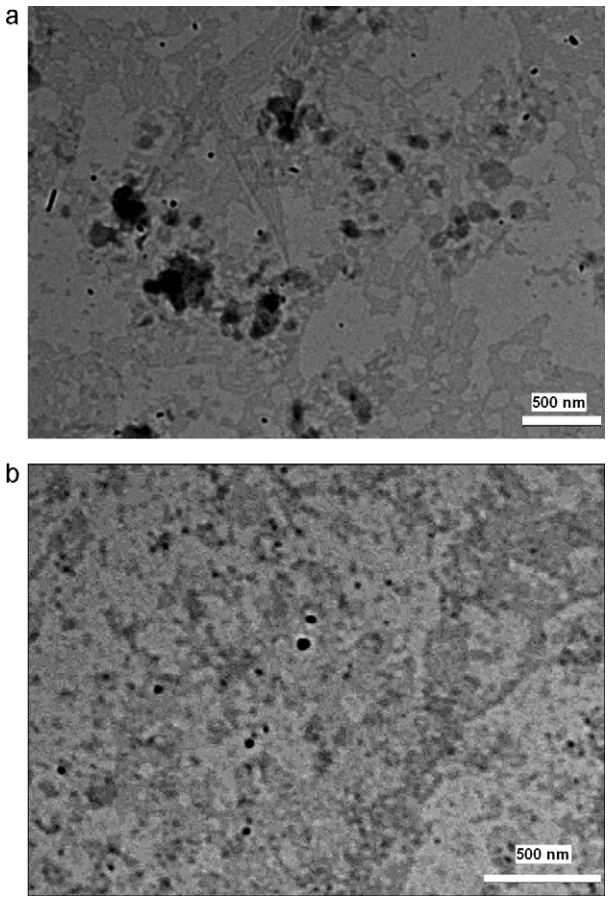

Fig. 4. (a) TEM image of silver nanoparticles obtained in microreactor (For $AgNO_3$ and $NaBH_4$ the total flow rate of addition of the precursor were maintained at 4 mL/min, $AgNO_3$ was 1 mL/min and $NaBH_4$ was 3 mL/min, 1:3 ratio). (b) TEM image of silver nano particles obtained in batch reactor.

of obtained in batch reactor were large in size. A number of articles found which have reported the effect of peak width at half maximum (PWHM) and its effect on particle size obtained in batch process. It has been reported that, with reduction in the PWHM value, there is decrease in particle size obtained in batch reactor. Kamat et al. [32] have reported batch process in which they obtained particle size of silver nanoparticles between 35 and 50 nm with PWHM at 100–110 nm. While Soloman et al. [36] have carried out experiments in batch reactor; they reported the PWHM value at 395–405 nm and the particle size in the range of 10–14 nm. In present study, using microreactor, it is possible to obtain the particle size in the range of 3–7 nm with PWHM 69. The results also indicate that the particle size obtained through microreactors has narrow particle size distribution compared with batch synthesis process [33–36].

3.3. Analysis of residence time distribution data (RTD) of microreactor

The analysis of the residence time distribution (RTD) of microreactor provides essential information about their overall performance. The residence time and RTD have a direct impact on the reaction process in microreactors due to the underlying reaction kinetics. In the typical flow range, viscous forces prevail over inertial forces which are indicated by low Reynolds numbers. The microreactor was characterized at various flow rates in the range 3–7 mL/min. For a detailed examination and interpretation of the RTD's obtained from modeling, some common notations and parameters are useful. It is convenient to display the RTDs in dimensionless form by using the dimensionless time θ to ensure a better comparability of measurements of different devices at different conditions [37,38] (Fig. 5a).

$$E(\theta) = \tau E(t) \tag{2}$$

$$\text{With} \quad \theta = \frac{t}{\tau} \tag{3}$$

where $\bar{t}$ is the mean residence time that can be obtained either directly from the model function or by numerical evaluation of the first moment of the RTD curve obtained, according to:

$$\tau = \int_0^\infty tE(t)dt \tag{4}$$

$$\tau = \bar{t} \tag{5}$$

The second central moment, the variance, is a useful parameter describing the width of a distribution and can be evaluated by:

$$\sigma^2 = \int_0^\infty (1-\tau)^2 E(t)dt \tag{6}$$

The experimental results of RTD are shown in Fig. 5a. The RTD obtained are narrow but show different shapes in terms of spread and symmetry. At high flow rates the RTD are narrow but broaden at lower flow rates. Additionally, asymmetry increases at lower flow rates and the maximum of the curves shifts to shorter dimensionless times. The RTD results represent deviation of microreactor from ideal plug flow. This deviation is due to the axial dispersion, however the narrower the RTD lower the axial dispersion. At low flow rates, the mixing efficiency of the mixing structure is low. Transversal mixing is governed by the slow process of molecular diffusion [37,38]. The dependence of the RTD on the flow rate can be more clearly derived from the dimensionless variance curve as shown in Fig. 5b. As the residence time at 3 mL/min is rather long, significant radial mixing occurs, by limiting the axial dispersion and leading to a low variance. In this study it is found that, at higher flow rates in the range between 3 and 7 mL/min, the mean residence time is shorter and therefore transversal mixing, due to diffusion is limited. The values of the variance increase, indicating less transversal mixing. Fig. 5c shows experimental residence time as a function of flow rate. The observed residence time at 3 mL/min flow rate is 0.65 min and it is found to decrease with an increase in the flow rate. The residence time at 7 mL/min flow rate is 0.28 min.

Fluid particles at different radial positions are spread and can no longer be mixed. The axial dispersion [37,38] is characterized by the axial Peclet number Pe_{ax} [37,38] which is given by

$$Pe_{ax} = \frac{\bar{u}L}{D_{ax}} \tag{7}$$

where L is the characteristic channel length and D_{ax} is axial diffusion coefficient. Pe_{ax} is calculated from the statistical moments [37,38] by

$$\sigma = \frac{2}{Pe_{ax}} + \frac{2}{Pe_{ax}^2} \tag{8}$$

The Pe_{ax} against the Re number was plotted as shown in Fig. 5d, which shows the continuous increase in Pe_{ax} with increase in Re number due to smaller hydraulic diameter in the microreactor causing higher flow velocities and thus stronger inertial forces promoting convective mixing and secondary flows. The Pe_{ax} number was highest, 0.39 at Re number 67 (flow rate of 7 mL/min) which signifies less axial dispersion and therefore confirmed by the less broadening of the RTD (Fig. 5a) at higher flow rate. These are in consistent with the RTDs reported by Boškovic et al. [38].

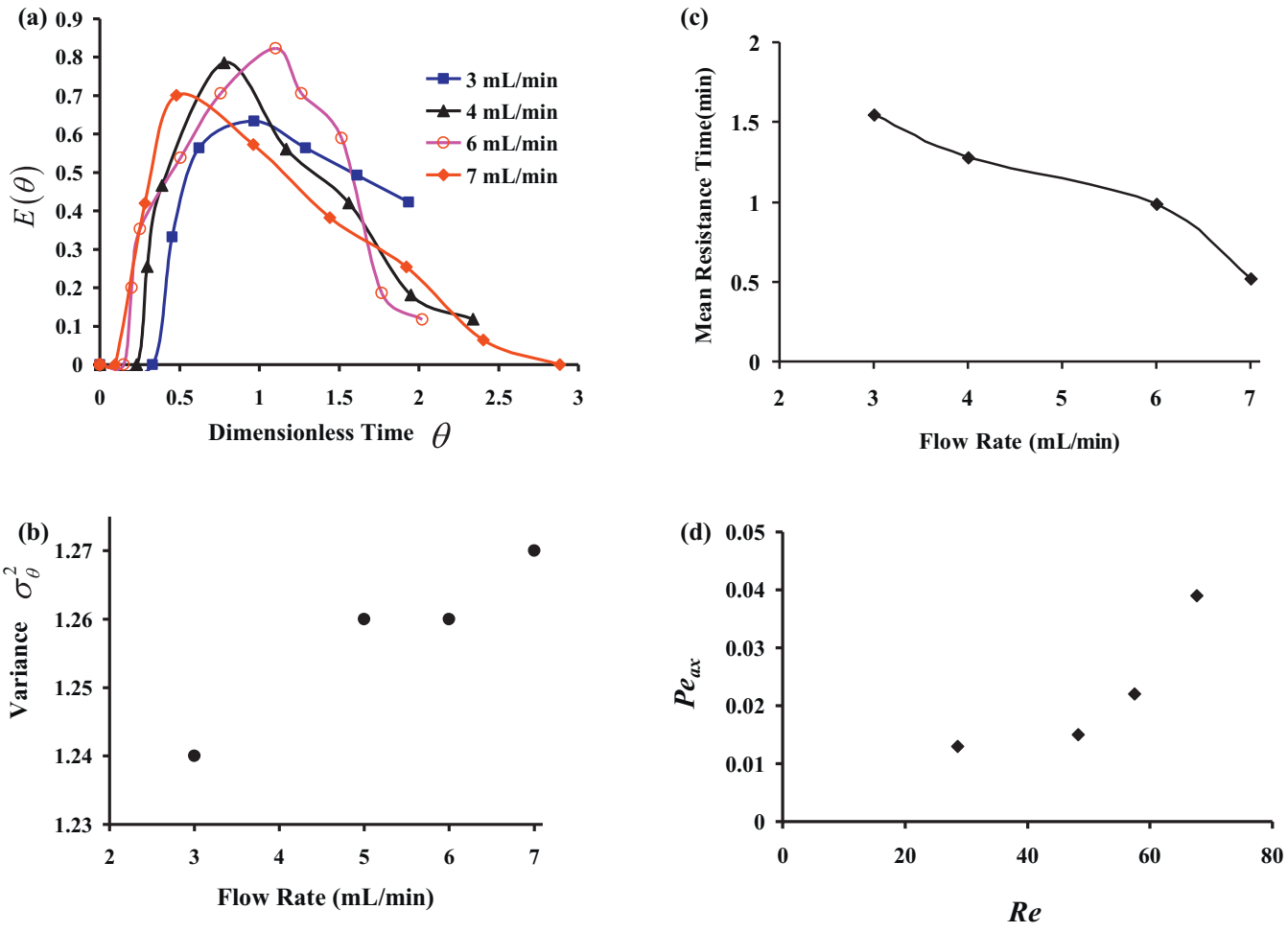

Fig. 5. RTD analysis of the microreactor for pulse input for flow rates varied between 3 and 7 mL/min.

3.4. *Effect of precursor concentration on particle size and optimization of sodium borohydride concentration*

To understand the effect of concentration of precursor ($AgNO_3$ and $NaBH_4$) on particle size, the total flow rate of addition of the precursor was maintained at 4 mL/min ($AgNO_3$ was 1 mL/min and $NaBH_4$ was 3 mL/min, 1:3 ratio) with space time $\tau = 0.48$ min and concentration of precursor was varied from 0.001 M to 0.005 M. Initially, it was found that, if the precursor ratio is maintained at 1:1 then no consistency in absorbance was observed. This might be due to the fact that there should be sufficient amount of sodium borohydride needed to reduce silver ion. Hence, the optimum ratio at 1:3 was maintained throughout the experimentation for microreactor based particle synthesis. All the experiments (Fig. 6) were carried out by addition of surfactant SDS at 9×10^{-3} mol/L. Fig. 6 depicts the UV spectrum of silver nanoparticles obtained at different precursor concentration. It was found that with increase in the precursor concentration the absorbance showed an increasing trend while the band width showed a decreasing trend. It was also observed that with decrease in the concentration of precursors from 0.005 M to 0.001 M, there is an increase in the PWHM value. Decrease in the concentration (i.e. diluted solutions) shows that decrement in absorbance value corresponds to the reduction in particle size. The absorption spectra show sharp absorbance peaks which are in the character range of surface plasma resonance peak of silver. The major reason for decreased intensity and broader width of absorption peaks were the electron surface scattering. For smaller particles electron reaches the surface faster and scatters quickly which results in broadening in absorption peak width. Table 1 summarizes the absorbance value at different initial feed concentration. For concentration 0.001 M absorbance was 0.578 a.u. while for 0.005 M absorbance value was 2.610 a.u.

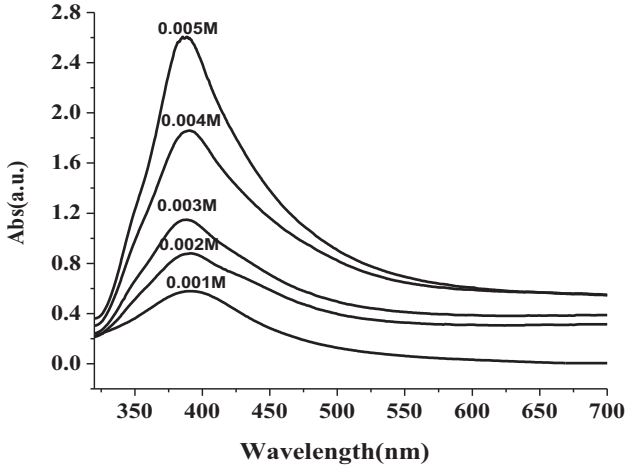

Fig. 6. UV absorption spectrum effect of different concentration and same flowrate of both reactants in microreactor. (Total flow rate of both the precursor (1:3 ratio of $AgNO_3$ and $NaBH_4$) were maintained at 4 mL/min and space time of the reactor was kept $\tau = 0.48$ min. surfactant SDS at 9×10^{-3} mol/L)

Table 1
Effect of concentration of reactants on absorbance value obtained in UV spectrophotometer analysis.

Concentration (1:1)	Absorbance (a.u.)
0.001 M	0.578
0.002 M	0.879
0.003 M	1.148
0.004 M	1.860
0.005 M	2.610

3.5. Study of kinetics of nucleation and growth of silver nano particles along the length of microreactor

Nucleation and growth of the silver nano particles was studied along the path in microreactor. In case of nanoscale metal particles, the absorption wavelength associated with the s–p transitions depends on the shape and size of the particle. For colloidal silver particles, larger and more asymmetric particles absorb at longer wavelengths than smaller, more spherical, particles [39].

Table 2 shows the representative sets of absorbance value and the λ_{max} (nm) shift of the solution as a function of path length/different longitudinal distances for two different concentrations – 0.003 M and 0.005 M. There is a similar trend in the absorbance value for both the silver nitrate concentrations. The initial drop in the absorbance value indicates the formation of nuclei (formation of solid phase as a result of super saturation) which corresponds to the drop in the ion concentration. After certain length, second stage, i.e. growth of the particle starts which finally gives stable particle size. The absorbance value decreases at 34 cm because the Ag^+ ion available by further reduction of silver nitrate causes rapid growth and lowers the concentration below the nucleation level while allowing the particles to grow further. Agglomeration of nano particles may lead to increase in overall particle size after certain length. The absorbance was obtained in the range of 399–420 nm suggesting that particles are of small size which is further confirmed by PSD analysis.

The absorbance was obtained in the range of 399–420 nm suggesting that particles are of small size, which is further confirmed by PSD analysis.

3.6. Effect of feed flow rate of precursor concentration

To determine the effect of feed flow rate on the particle size, feed flow rates from 1 to 4 mL/min were maintained and the resulting absorbance values were estimated. To identify the effect of flow rate, the variation in flow rate was carried out from 1 to 3 mL/min (total flow rate of both precursors) by keeping other parameter constant and concentration of silver nitrate to sodium borohydride was kept at 1:3 ratio. As shown in Fig. 7, it is found that the flow rate could affect the size of silver nanoparticles. With increase in flow rates, UV absorbance shows the broadening of the peak. As shown in Table 3, with increase in the flow rate the PWHM value an increase which indicates that the particle size increases. This is confirmed by TEM images which also indicate irregularity of particles increases with the increase in flow rate as shown in Fig. 4. Kumar et al. [40] have reported that the flow rate should be

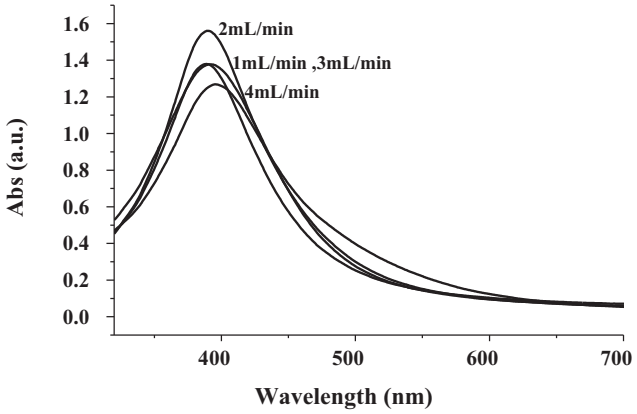

Fig. 7. UV absorption spectrum at various flow rates having 1:3 proportions of reactants.

Table 3
Effect of flow rates on λ_{max}, PWHM values and the absorbance of Ag^0 nanoparticles.

Flow rates (mL/min)	λ_{max} (nm)	Absorbance (a.u.)	PWHM (nm)
1	388.40	1.380	107.5
2	390.50	1.560	92
3	392	1.378	119
4	395.50	1.268	128.5

maximum for getting narrow particle size distribution but overall particle size is higher at higher flow rate. Due to fast flow of reaction mixture into microreactor, there is less residence time for nucleation, but there is sufficient time for coalescence of the newly formed nanoparticles. Hence at higher flow rate the particle size is found to be higher. To get complete formation of nanoparticles, sufficient amount of reducing agent is needed which can be finely tuned by using flow rate of silver nitrate and sodium borohydride. This will lead to formation of fine and monodisperse nanoparticles. 2 mL/min was the optimum flow rate at which reaction gets completed within 2 min without aggregation of particles. Broadening in absorbance spectrum suggests that the nanoparticles become polydisperse [41,42]. As shown in Table 3, by increasing the flow rate a decrease in absorbance and thereby an increase in PWHM value were observed, which leads to increase in the particle size. For the optimum flow rate of 2 mL/min the observed absorbance value was 1.560, while for PWHM the observed absorbance value was 92. It is important to note that 2 mL/min flow rate is optimum for obtaining monodisperse nanoparticles than other flow rates. Increasing value of λ_{max} with increase in flow rates indicates that the λ_{max} is dependent on flow rates. Higher flow rate leads to cluster formation hence there should not be excess flow rates than the optimum.

3.7. Effect of surfactant type onto the silver nanoparticle synthesis in microreactor

Comparative study of intensification colloidal synthesis by the addition of different surfactant is important as surface charges on particles are influenced by type of surfactant (anionic/cationic).

Table 2
Study of nucleation and growth of nano particles along the length of microreactor.

Sr. no.	$AgNO_3$ (M)	0.005				0.003			
	$NaBH_4$ (M)	0.015				0.009			
1	Sampling distance from inlet (cm)	1.5	19.5	34	102	1.5	19.5	34	102
2	λ_{max} (nm) shift of the solution at different distance	412	413	412	404	407	403	399	402
3	Absorbance (a.u.) value of solution in microreactor at different lengths	0.32	1.2	0.6	0.44	0.62	1.30	0.20	0.38

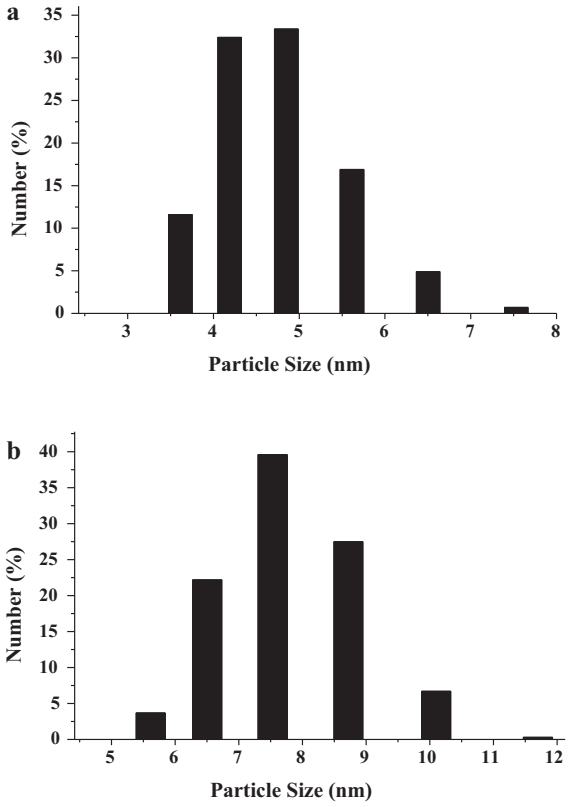

Fig. 8. (a) Histogram of particle size analyzer for silver nanoparticles using SDS as surfactant in microreactor. (b) Histogram of particle size analyzer for silver nanoparticles using SDS as surfactant in batch process.

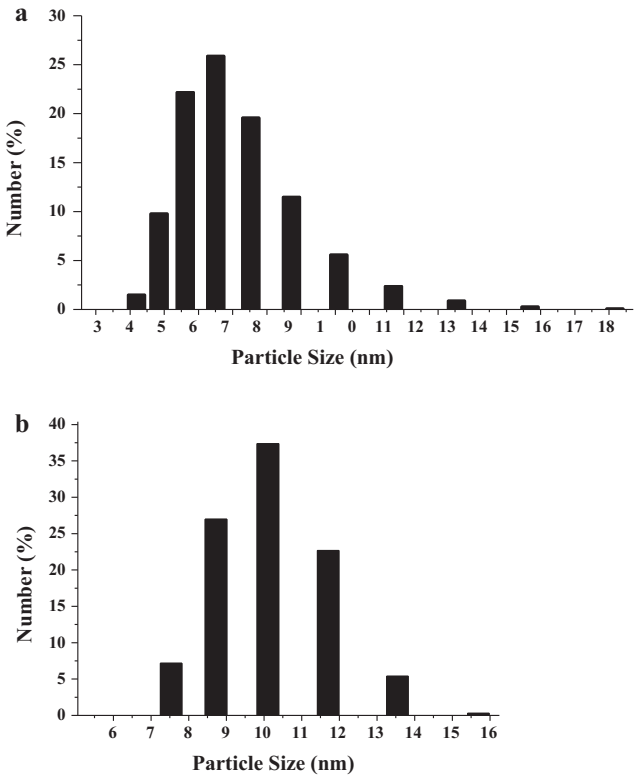

Fig. 9. (a) Histogram of particle size analyzer for silver nanoparticles using CTAB as surfactant in microreactor. (b) Histogram of particle size analyzer for silver nanoparticles using CTAB as surfactant in batch process.

Two surfactants namely sodium dodecyl sulfate (SDS) and N-cetyl N,N,N,trimethyl ammonium bromide (CTAB) were identified for experimental investigation. Adsorbed borohydride provides particle surface charge and stabilizes growing silver nanoparticles. However, there is much possibility of aggregation during synthesis of silver nanoparticles without SDS surfactant. SDS is the anionic surfactant having negative charge on head. Repulsive forces due to presence of negative BH^- charges on micelles avoid the cluster formation of silver nanoparticles and thus finally, get small nanoparticle size. Surfactant provides a cage like effect that can control nucleation and growth of nanoparticles. CTAB is a cationic surfactant having positive charge on head. Fig. 8a presents the particle size distribution histogram for silver nanoparticles in microreactor in which $AgNO_3$ flow rate was 1 mL/min (0.001 M) and $NaBH_4$ was 3 mL/min (0.003 M) used. SDS surfactant was added in both precursors. Fig. 8a shows that average particle size distribution at this condition was 4.8 nm. Fig. 8b indicates particle size distribution of silver nanoparticles synthesized by batch process using SDS surfactant. Quantity of sodium borohydride added was 60 mL (0.002 M) and silver nitrate was 20 mL (0.001 M). For batch process the average particle size was found in the range of 7.5 nm. For comparison purpose similar experiments were carried out with CTAB as surfactant, which is reported in Fig. 9. As shown in Fig. 9a, synthesis was carried out using microreactor at flow rate of $NaBH_4$ of 3 mL/min (0.002 M) and silver nitrate at 1 mL/min (0.001 M). The particle size distribution observed was in wide range from 4 to 18 nm. Fig. 9b, histogram shows particle size of silver nanoparticle synthesized in batch process. In the batch process 60 mL sodium borohydride (0.002 M) and 20 mL silver nitrate (0.001 M) were added. Surfactant CTAB was added in both solutions. In batch process, particle size was in the range of 7–16 nm.

3.8. Effect of surfactant loading onto the silver nanoparticle synthesis in microreactor

The effect of surfactant loading (SDS and CTAB) is depicted in Fig. 10. To study the effect of surfactant loading on particle size, the total flow rate of addition of the precursor was maintained at 4 mL/min ($AgNO_3$ was 1 mL/min and $NaBH_4$ = 3 mL/min, 1:3 ratio) with space time τ = 0.48 min. The concentration of precursor was maintained at 0.001 M $AgNO_3$ and 0.003 M $NaBH_4$ during the study of effect of loading of surfactant. Fig. 10a reports the effect of the SDS loading on absorbance. It is found that with an increase in the SDS loading the absorbance shows increasing trend upto 0.09 g SDS loading and then it is found to decrease with an increase in the SDS loading. Table 4 also reports the effect of SDS loading on λ_{max}, PWHM values and the absorbance of Ag^0 nanoparticles. It is observed that the λ_{max} and absorbance value are increased from 425.3 to 434.4 nm and 0.241 to 1.166 a.u. respectively with an increase in the SDS loading from 0.05 to 0.09 g, whereas these

Table 4
Effect of surfactant loading on λ_{max}, PWHM values and the absorbance of Ag^0 nanoparticles.

Surfactant loading (g)	λ_{max} (nm)	Absorbance (a.u.)	PWHM (nm)
SDS			
0.05	425.3	0.241	129.8
0.07	420.0	0.273	99.40
0.09	434.4	1.166	112.4
0.11	429.9	0.608	95.80
CTAB			
0.1	425.4	2.385	67.10
0.2	425.4	0.881	89.90
0.3	443.0	0.407	116.6
0.4	431.8	0.373	120.3

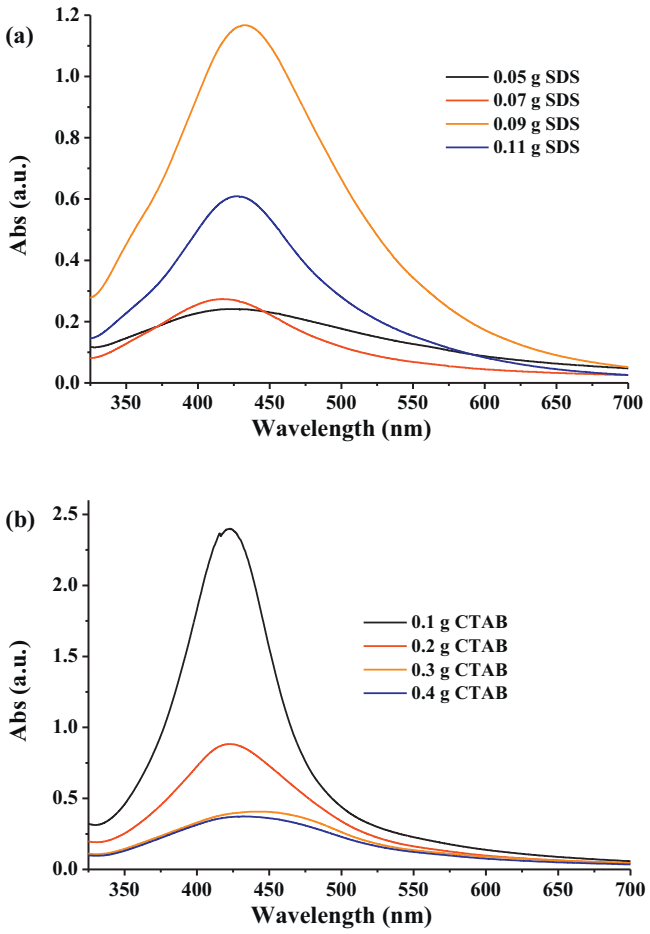

Fig. 10. UV absorption spectrum at various surfactant concentrations having 1:3 proportions of reactants (a) SDS and (b) CTAB.

values are found to decrease at 0.11 g SDS loading. The PWHM values are in the range of 95.80–129.8 nm for different SDS loading. This clearly indicates that an increase in the SDS loading results in increase in the number of nuclei formation which in turn leads to reduction in the particle size of Ag nanoparticles. Further, presence of negative charge on head of SDS molecule leads to repulsion of negative BH^- charges on micelles, which avoids the agglomeration of silver nanoparticles results into smaller nanoparticle size. Fig. 10b depicts the effect of the CTAB loading on absorbance. The absorbance was found to decrease with an increase in the CTAB loading. Table 4 also reports the effect of CTAB loading on λ_{max}, PWHM values and the absorbance of Ag^0 nanoparticles. The λ_{max} and PWHM value was found to increase from 425.4 to 431.8 nm and 67.1 to 120.3 nm respectively with an increase in the CTAB loading from 0.1 to 0.4 g, whereas absorbance was found to be decreased. In general, as the particles become larger the absorption maximum shifts to longer wavelengths and the peaks broaden [43]. In this work the shifting of λ_{max} value to larger side and broadening of peak (indicated by increase in PWHM value) shows an increase in the Ag nanoparticle size. The absorbance value was found to decrease with an increase in the CTAB loading. This indicates low CTAB loading favors the formation of a large number of nuclei, whereas it gets decreased with an increase in the CTAB loading. The increase in the particle size with an increase in the CTAB loading is due to the agglomeration effect that cationic CTAB, which has positive charge on head, favors. These results and discussion are consistent with the results reported in the earlier section.

4. Conclusions

Synthesis of silver nanoparticles in microreactor and batch reactor by using sodium borohydride and silver nitrate were carried out. The optimum conditions and parameters for microreactor was identified and maintained. Microreactor in which $AgNO_3$ flow rate was 1 mL/min (0.001 M) and $NaBH_4$ was 3 mL/min (0.003 M) shows minimum particle size of 4.8 nm. Further effect of SDS and CTAB as well as comparative study in batch and microreactor was carried out. It is found that optimum flow conditions and concentration of SDS surfactant (0.02 g/mL) will help to generate mono dispersed nanoparticles. It is successfully demonstrated that using microreactor, monodispersed, nano size (3–7 nm) silver nanoparticles were synthesized at optimum process conditions. It is also observed that with the simple experimental setup, nano particles with controlled size can be synthesized continuously using microreactor. PWHM value showed an increasing trend with increase in flow rates of reactants, and this indicates the possibility of polydisperse particles formation. The increase in the particle size with an increase in the CTAB loading is due to the agglomeration effect that cationic CTAB, which has positive charge on head, favors. The RTD behavior of microreactor was successfully analyzed by employing a pulse input to microreactor at different flow rates of fluid.

Acknowledgements

Author acknowledges University Grant Commission (UGC) New Delhi for financial support though grant number 39–1014/2010 (SR). Authors are thankful to Mr. Anand Gole and Sumant Phadtare of Tata Chemicals, Pune for their help in Particle Size Distribution Analysis. Authors are also thankful to Mr. S.A. Ghodke and Mr. Laxmikant Bhagwat for there help in experimental.

References

[1] P. Mukherjee, C.R. Patra, A. Ghosh, R. Kumar, M. Sastry, Characterization and catalytic activity of gold nanoparticles synthesized by autoreduction of aqueous chloroaurate ions with fumed silica, Chemistry of Materials 14 (2002) 1678–1684.
[2] J.M. Kohler, A. Csaki, J. Reichert, R. Moller, W. Straube, W. Fritzsche, Selective labeling of oligonucleotide monolayers by metallic nanobeads for fast optical readout of DNA-chips, Sensors and Actuators B 76 (2001) 166–172.
[3] A. Henglein, Colloidal silver nanoparticles: photochemical preparation and interaction with O_2, CCl_4, and some metal ions, Chemistry of Materials 10 (1998) 444–450.
[4] N. Nath, A. Chilkoti, A colorimetric gold nanoparticle sensor to interrogate biomolecular interactions in real time on a surface, Analytical Chemistry 74 (2002) 504–509.
[5] C.X. Zhao, L. He, S.Z. Qiao, A.P.J. Middelberg, Nanoparticle synthesis in microreactors, Chemical Engineering Science 66 (2011) 1463–1479.
[6] C.N.R. Rao, G.U. Kulkarni, P.J. Thomasa, P.P. Edwards, Metal nanoparticles and their assemblies, Chemical Society Reviews 29 (2000) 27–35.
[7] A.J. deMello, Control and detection of chemical reactions in microfluidic systems, Nature 442 (2006) 394–402.
[8] A. Jahn, J.E. Reiner, W.N. Vreeland, D.L. DeVoe, L.E. Locascio, M. Gaitan, Preparation of nanoparticles by continuous flow microfluidics, Journal of Nanoparticle Research 10 (2008) 925–934.
[9] L.R. Arana, S.B. Schaevitz, A.J. Franz, M.A. Schmidt, K.F. Jensen, A microfabricated suspended tube chemical reactor for thermally efficient fuel processing, Journal of Microelectromechanical Systems 12 (2003) 600–612.
[10] J. Kobayashi, Y. Mori, K. Okamoto, R. Akiyama, M. Ueno, T. Kitamori, S. Kobayashi, A microfluidic device for conducting gas–liquid–solid hydrogenation reactions, Science 304 (2004) 1305–1308.
[11] E.M. Chan, R.A. Mathies, A.P. Alivisatoes, Size controlled growth of CdSe nanocrystals in microfluidic reactors, Nano Letters 3 (2003) 199–201.
[12] H. Nakamura, Y. Yamaguchi, M. Miyzaki, H. Maeda, M. Uehara, P. Muivanay, Preparation of CdSe nanocrystals in a micro-flow-reactor, Chemical Communications 15 (2002) 2844–2845.
[13] B.K.H. Yen, N.E. Stott, K.F. Jensen, M.G. Bawendi, A continuous-flow microcapillary reactor for the preparation of a size series of CdSe nanocrystals, Advanced Materials 15 (2003) 1858–1862.
[14] I. Shestpalov, J.D. Tice, R.F. Ismagilov, Multistep synthesis of nanoparticles performed on millisecond time scale in a microfluidics droplet based system, Lab on a Chip 4 (2004) 316–321.

[15] H. Wang, H. Nakamura, M. Uehara, M. Miyazaki, H. Maeda, Preparation of titania particles utilizing the insoluble phase interface in microchannel reactor, Chemical Communications (Cambridge, England) 15 (2002) 1462–1463.
[16] S.T. He, T. Kohira, M. Uehara, T. Kitamura, H. Nakamura, M. Miyazaki, Effect of interior wall on continuous fabrication of silver nanoparticles in micro capillary reactor, Chemistry Letters 34 (2005) 748–749.
[17] J. Boleininger, A. Kurz, V. Reuss, C. Sönnichsen, Microfluidic continuous flow synthesis of rod-shaped gold and silver nanocrystals, Physical Chemistry Chemical Physics 8 (2006) 3824–3827.
[18] X.Z. Lin, A.D. Terepka, H. Yang, Synthesis of silver nanoparticles in a continuous flow tubular microreactor, Nano Letters 4 (2004) 2227–2232.
[19] A. Singh, M. Shirolkar, N.P. Lalla, C.K. Malek, S.K. Kulkarni, Room temperature, water-based, microreactor synthesis of gold and silver nanoparticles, International Journal of Nanotechnology 6 (2009) 541–551.
[20] J. Wagner, J.M. Köhler, Continuous synthesis of gold nanoparticles in a microreactor, Nano Letters 5 (2005) 685–691.
[21] J. Wagner, T. Kirner, G. Mayer, J. Albert, J.M. Köhler, Generation of metal nanoparticles in a microchannel reactor, Chemical Engineering Journal 101 (2004) 251–260.
[22] H. Nishikawa, T. Morita, J. Sugiyama, S. Kimura, Formation of gold nanoparticles in microreactor composed of helical peptide assembly in water, Journal of Colloid and Interface Science 280 (2004) 506–510.
[23] J.B. Edel, R. Fortt, J.C. deMello, A.J. deMello, Microfluidic routes to the controlled production of nanoparticles, Chemical Communications 10 (2002) 1136–1137.
[24] K.S. Huang, T.H. Lai, Y.C. Lin, Manipulating the generation of Ca-alginate microspheres using microfluidic channels as a carrier of gold nanoparticles, Lab on a Chip 6 (2006) 954–957.
[25] S.A. Khan, A. Gunther, M.A. Schmidt, K.F. Jensen, Microfluidic synthesis of colloidal silica, Langmuir 20 (2004) 8604–8611.
[26] A. Kück, M. Steinfeldt, K. Prenzel, P. Swiderek, A.v. Gleich, J. Thöming, Green nanoparticle production using micro reactor technology, Journal of Physics: Conference Series 304 (2011), 012074, 1–10.
[27] D. Jeevarathinam, A.K. Gupta, B. Pitchumani, R. Mohan, Effect of gas and liquid flowrates on the size distribution of barium sulfate nanoparticles precipitated in a two phase flow capillary microreactor, Chemical Engineering Journal 173 (2011) 607–611.
[28] J. Wang, I. Alfredo, M.P. Chatrathi, On chip integration of enzyme and immunoassays: simultaneous measurements of insulin and glucose, Journal of the American Chemical Society 125 (2003) 8444–8445.
[29] I.P. Santos, L.M. Liz-Marzán, Formation of PVP-protected metal nanoparticles in DMF, Langmuir 18 (2002) 2888–2894.
[30] L.M. Liz-Marzán, I.L. Touriño, Reduction and stabilization of silver nanoparticles in ethanol by nonionic surfactants, Langmuir 12 (1996) 3585–3589.
[31] Y. Xiong, I. Washio, J. Chen, M. Sadilek, Y. Xia, Trimeric clusters of silver in aqueous $AgNO_3$ solutions and their role as nuclei in forming triangular nanoplates of silver, Angewandte Chemie International Edition in English 46 (2007) 4917–4921.
[32] P.V. Kamat, M. Flumiani, G.V. Hartland, Picosecond dynamics of silver nanoclusters. Photoejection of electrons and fragmentation, Journal of Physical Chemistry B 102 (1998) 3123–3128.
[33] A. Zanzotto, N. Szita, P. Boccazzi, P. Lessard, A.J. Sinskey, K.F. Jensen, Membrane-aerated microbioreactor for high-throughput bioprocessing, Biotechnology and Bioengineering 87 (2004) 243–254.
[34] X. Zhang, S. Stefanick, F.J. Villani, Application of microreactor technology in process development, Organic Process Research and Development 8 (2004) 455–460.
[35] A.S. Nair, T.Y. Pradeep, Halocarbon mineralization and catalytic destruction by metal nanoparticles, Current Science 84 (2003) 1560–1564.
[36] L. Mulfinger, S.D. Soloman, M. Bahadory, A.V. Jeyarajasingam, S.A. Rutkowsky, C. Boritz, Synthesis and study of silver nanoparticles, Journal of Chemical Education 84 (2007) 322–325.
[37] H. Scott Fogler, Elements of Chemical Reaction Engineering, 4th ed., Prentice Hall, New Jersey, 2005.
[38] D. Boškovic, S. Löbbecke, A. Groß, M. Köhler, Residence time distribution studies in microfluidic mixing structures, Chemical Engineering and Technology 34 (2011) 361–370.
[39] V.K. LaMer, R.H. Dinegar, Theory, production and mechanism of formation of mono dispersed hydrosols, Journal of the American Chemical Society 72 (1950) 4847–4854.
[40] D.V.R. Kumar, M. Kasture, A.A. Prabhune, C.V. Ramana, B.L.V. Prasad, A.A. Kulkarni, Continuous flow synthesis of functionalized silver nanoparticles using bifunctional biosurfactants, Green Chemistry 12 (2010) 609–615.
[41] S.T. He, Y.L. Liu, H. Maeda, Controlled synthesis of colloidal silver nanoparticles in capillary micro-flow reactor, Journal of Nanoparticle Research 10 (2008) 209–215.
[42] S. Quintillan, C. Tojo, M.C. Blanco, M.A. Lopez-Quintela, Effect of the intermicellar exchange on the size control of nanoparticles synthesized in microemulsions, Langmuir 17 (2001) 7251–7254.
[43] M. Bahadory, Synthesis of noble metal nanoparticles, Ph.D. Thesis, Drexel University, August 2008.